Article

Cell Reports

Cell-Autonomous Regulation of Mu-Opioid Receptor Recycling by Substance P

Graphical Abstract

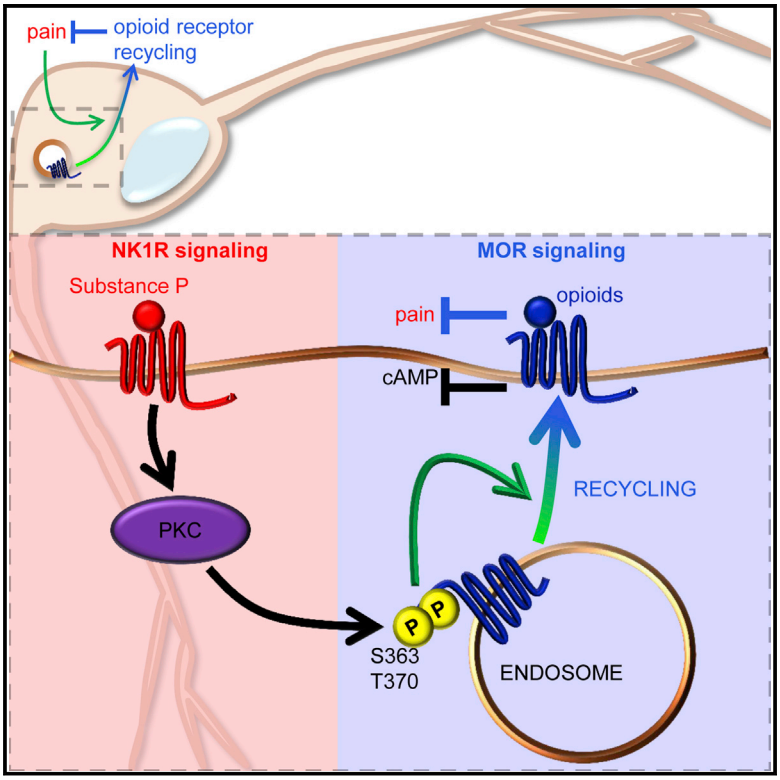

Authors

Shanna L. Bowman, Amanda L. Soohoo, ..., Amynah A. Pradhan, Manojkumar A. Puthenveedu

Correspondence

map3@andrew.cmu.edu

In Brief

Bowman et al. show that substance P (SP), acting through the NK1 receptor, increases recycling of mu-opioid receptors (MORs) after fentanyl, but not morphine. This increase requires PKC-mediated phosphorylation of MOR. Furthermore, SP increases neuronal sensitivity to opioids and reduces acute tolerance to fentanyl, but not morphine. This suggests a mechanism for crosstalk between inflammatory pain and opioid analgesia.

Highlights

- Substance P increases recycling of mu-opioid receptors in sensory neurons
- PKC activation via NK1 receptor is required and sufficient for this crosstalk
- The crosstalk is mediated by direct MOR phosphorylation at two discrete sites
- SP and PKC regulate neuronal resensitization and opioid antinociception in mice

Bowman et al., 2015, Cell Reports *10*, 1925–1936
March 24, 2015 ©2015 The Authors
http://dx.doi.org/10.1016/j.celrep.2015.02.045

Cell Reports
Article

Cell-Autonomous Regulation of Mu-Opioid Receptor Recycling by Substance P

Shanna L. Bowman,[1,4] Amanda L. Soohoo,[1,4] Daniel J. Shiwarski,[1] Stefan Schulz,[2] Amynah A. Pradhan,[3] and Manojkumar A. Puthenveedu[1,*]
[1]Department of Biological Sciences, Carnegie Mellon University, 4400 Fifth Avenue, Pittsburgh, PA 15213, USA
[2]Institute of Pharmacology and Toxicology, Jena University Hospital, Friedrich Schiller University Jena, Drackendorfer Straße 1, 07747 Jena, Germany
[3]Department of Psychiatry, University of Illinois, Chicago, 1601 West Taylor Street, Chicago, IL 60612, USA
[4]Co-first author
*Correspondence: map3@andrew.cmu.edu
http://dx.doi.org/10.1016/j.celrep.2015.02.045

SUMMARY

How neurons coordinate and reprogram multiple neurotransmitter signals is an area of broad interest. Here, we show that substance P (SP), a neuropeptide associated with inflammatory pain, reprograms opioid receptor recycling and signaling. SP, through activation of the neurokinin 1 (NK1R) receptor, increases the post-endocytic recycling of the mu-opioid receptor (MOR) in trigeminal ganglion (TG) neurons in an agonist-selective manner. SP-mediated protein kinase C (PKC) activation is both required and sufficient for increasing recycling of exogenous and endogenous MOR in TG neurons. The target of this cross-regulation is MOR itself, given that mutation of either of two PKC phosphorylation sites on MOR abolishes the SP-induced increase in recycling and resensitization. Furthermore, SP enhances the resensitization of fentanyl-induced, but not morphine-induced, antinociception in mice. Our results define a physiological pathway that cross-regulates opioid receptor recycling via direct modification of MOR and suggest a mode of homeostatic interaction between the pain and analgesic systems.

INTRODUCTION

Most neurotransmitter signals are transduced by G protein-coupled receptors (GPCRs), the largest family of signaling receptors (Pierce et al., 2002; Rosenbaum et al., 2009; Premont and Gainetdinov, 2007; Shepherd and Huganir, 2007; von Zastrow and Williams, 2012). The strength of a neuronal response directly depends on surface receptor numbers. Therefore, regulation of this number via membrane trafficking is critical for modulating neuronal responsiveness to a given signal (Anggono and Huganir, 2012; Gainetdinov et al., 2004; Marchese et al., 2008; Yudowski et al., 2009). It is accepted that membrane trafficking can control the number of surface receptors and therefore signaling, and many mechanisms have been identified. Emerging evidence suggests that signaling also can control membrane trafficking, but the mechanisms that underlie such crosstalk are still largely unresolved (Jean-Alphonse and Hanyaloglu, 2011).

Post-endocytic receptor sorting, a trafficking step critical for receptor physiology (Sorkin and von Zastrow, 2009; Anggono and Huganir, 2012; Marchese et al., 2008; Scita and Di Fiore, 2010; Williams et al., 2013), provides a potential point for such crosstalk. Activated surface receptors are rapidly internalized by clathrin-mediated endocytosis and transported to the endosome, causing receptor removal from the cell surface, which is associated with a loss of cellular sensitivity (Alvarez et al., 2002; Claing et al., 2002; Hanyaloglu and von Zastrow, 2007; Keith et al., 1996; Martini and Whistler, 2007). Cellular sensitivity to further extracellular signals is then determined by post-endocytic receptor sorting between the degradative and recycling pathways, as small changes in recycling rates can cause relatively large changes in surface receptor numbers over physiological timescales (Sorkin and von Zastrow, 2009; Arttamangkul et al., 2012; Jean-Alphonse and Hanyaloglu, 2011; von Zastrow and Williams, 2012). How receptor recycling is controlled by heterologous signaling pathways in a physiological context is a fundamental question that is still not very well understood (Marchese et al., 2008; Williams et al., 2013).

Here we focused on two signaling pathways that functionally interact—pain and analgesia—as physiologically relevant examples for potential signaling crosstalk. Pain in nociceptive neurons is associated with activation of the neurokinin 1 receptor (NK1R) by substance P (SP) (Perl, 2007; De Felipe et al., 1998), while analgesia is primarily mediated by opioids via the mu-opioid receptor (MOR) (Chen and Marvizón, 2009; Kieffer, 1995; Lao et al., 2008). We show that NK1R activation by SP increases MOR post-endocytic recycling in sensory neurons, via a cross-regulatory mechanism based on direct modification of MOR. NK1R signaling also increases the resensitization of MOR-mediated antinociception in mice. Our results provide a physiologically relevant example for crosstalk between signaling pathways at the level of receptor trafficking.

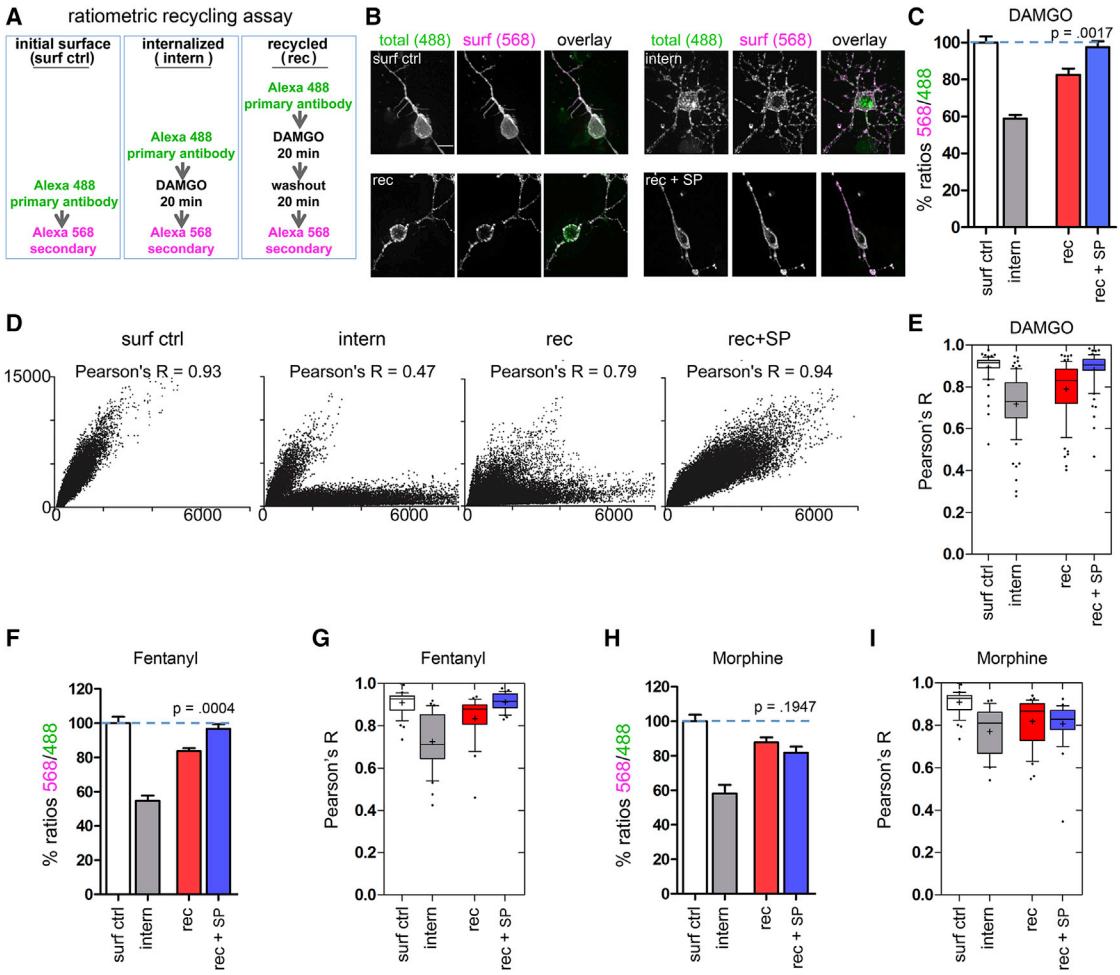

Figure 1. SP Increases Post-endocytic Recycling of MOR

(A) Schematic of the quantitative ratiometric recycling assay in TG neurons.

(B) Example images of FLAG-MOR in primary TG neurons: surface control (surf ctrl), internalization control (intern), DG washout (rec), and washout with SP (rec + SP). Primary anti-FLAG labeling showing the total pool of receptors initially on the surface (total 488) is green in the overlay. Secondary antibody labeling showing the fraction of the initial pool on the surface at the end of the treatment (surf 568) is red in the overlay. A ratio of the 568 to 488 fluorescence gives the fraction of the initial pool present on the surface at the end. Scale bar represents 10 μm.

(C) Percentage recycling calculated from the ratios of surface (568) to total (488) in each condition (mean ± SEM; n = 77 surf ctrl, 78 intern, 69 rec, and 68 rec + SP).

(D) Cytofluorograms showing pixel-level fluorescence correlation between total and surface-only pools. The surf ctrl shows strong correlation between the two channels; the intensity values trend to a single diagonal line. DG (intern) causes separation of the points into two populations, consistent with a decrease in colocalization because the anti-FLAG on internalized MOR is not accessible to the secondary antibodies. DG washout increases the correlation, which is further enhanced by SP. Pearson's correlation coefficients are shown for each example.

(E) Tukey box plots showing the first and third quartiles of the distribution of Pearson's coefficients across multiple cells (n as above). Middle bar shows the median, outside bars show 10th and 90th percentiles, and + shows the mean. Scale bars represent 5 μm.

(F) Percentage recycling increased during washout, following activation of TGs with fentanyl (n = 37 surf ctrl, 33 intern, 29 rec, and 38 rec + SP).

(G) Tukey box plots showing Pearson's coefficients from cells in (F).

(H) Percentage recycling increased during washout, following activation of TGs with morphine (n = 37 surf ctrl, 34 intern, 37 rec, and 30 rec + SP).

(I) Tukey box plots showing Pearson's coefficients from cells in (H).

All error bars are ±SEM.

RESULTS

SP Signaling through NK1R Increases Post-endocytic Recycling of MOR

To test if NK1R signaling cross-regulates MOR recycling, we chose trigeminal ganglia (TG) neurons as model cells. TG neurons are highly relevant for neuralgia, a common and severe pain disorder, and they endogenously express MOR and NK1R (Aicher et al., 2000). To measure MOR recycling, we used an assay to quantitate recycled FLAG-tagged MORs (Figure 1A). These tagged receptors were fully competent for signaling and trafficking, as reported previously (Arttamangkul

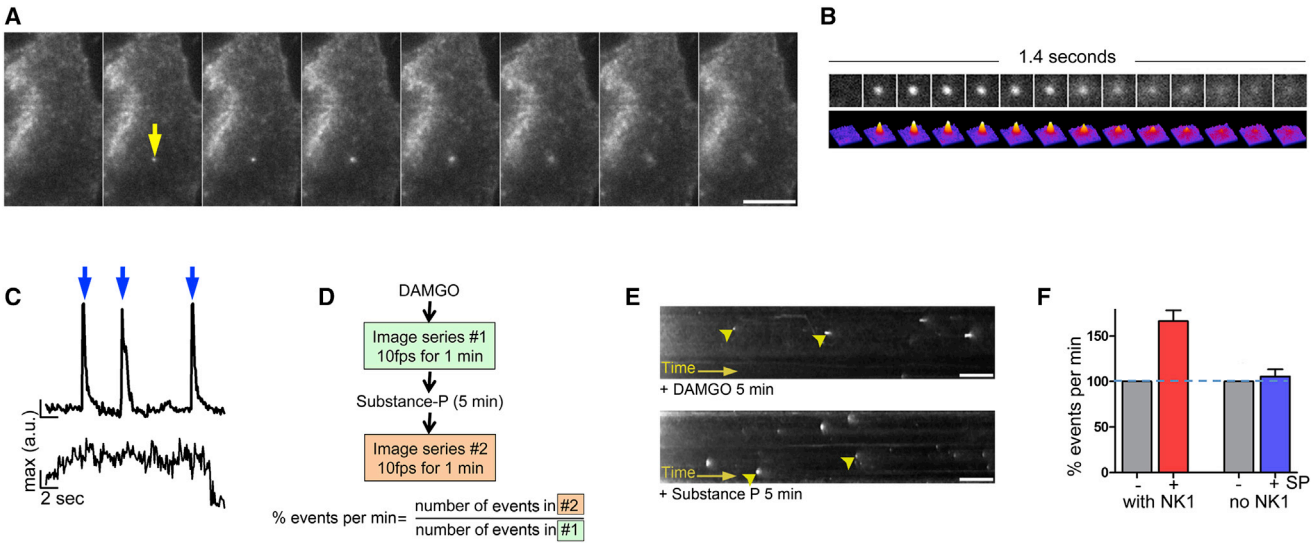

Figure 2. SP Signaling through NK1R Regulates Individual MOR Recycling Events

(A) Cells expressing SpH-MOR imaged with TIRF microscopy 5 min after DG addition. Frames are 100 ms apart. An individual exocytic event is indicated by yellow arrow. Scale bar represents 5 μm.

(B) Lifetime of an SpH-MOR exocytic event. Insertion events begin as a localized, intense burst of fluorescence that diffuses within a second. Heat map of intensity is shown below as a surface plot.

(C) Maximum intensity traces of an SpH-MOR vesicle exocytic event (top, arrows), showing characteristic rapid spikes and an endocytic cluster (bottom), which persists for much longer with a characteristic exponential decrease at the end.

(D) Experimental workflow to quantify acute regulation of recycling.

(E) Kymographs of SpH-MOR fusion events from the same region in the same cell, expressing both SpH-MOR and an HA-tagged NK1R, following sequential DG and SP addition. Arrowheads show exocytic events, which increase after SP. Scale bar represents 2 s.

(F) Number of SpH-MOR exocytic events per minute after SP addition normalized to before (i.e., with just DG) in cells expressing NK1R and in adjacent cells not expressing NK1R. Error bars are SEM (n = 20). See also Figure S1 and Movies S1, S2, and S3.

All error bars are ±SEM.

et al., 2008; Just et al., 2013; Keith et al., 1996; Soohoo and Puthenveedu, 2013). TG neurons expressing FLAG-MOR were labeled with fluorescent Alexa 488-conjugated anti-FLAG antibodies to detect the existing pool of MOR on the cell surface (Figure 1B, top left). MOR activation by the specific agonist [D-Ala2, N-MePhe4, Gly-ol]-enkephalin (DAMGO, noted as DG) induced robust MOR internalization, detected by the appearance of intracellular MOR fluorescence (Figure 1B, top right). DG was then washed out to allow MOR recycling. Next the cells were labeled by Alexa 568-conjugated secondary antibodies, which only label surface anti-FLAG-labeled MOR. MOR recycling was quantitated as the ratio of the secondary (surface) to primary (total) antibody fluorescence values. This ratiometric assay allowed us to differentiate recycling from the insertion of newly synthesized MOR. Activation of endogenous NK1Rs by SP during the agonist washout increased the ratio of surface to total fluorescence, indicating increased MOR recycling (Figures 1B [bottom] and 1C [right]; Hunt and Mantyh, 2001; Nichols et al., 1999; De Felipe et al., 1998).

We measured the pixel-based colocalization of the surface to total MOR by calculating the Pearson's correlation between the two fluorophores. Before DG, a strong correlation was observed, as seen in the cytofluorogram (e.g., cell in Figures 1D and 1E). After DG, colocalization decreased and two separate populations emerged, consistent with MOR endocytosis and decreased labeling with the secondary antibody on the surface (Figures 1D and 1E). Colocalization increased when SP was added to the washout (Figure 1E), suggesting an increase in surface MOR. We next asked if SP was capable of regulating MOR recycling when MORs were stimulated with two clinically relevant opioids, fentanyl and morphine. SP increased MOR recycling after endocytosis induced by fentanyl (Figures 1F and 1G), but not morphine (Figures 1H and 1I).

To directly visualize and quantify MOR recycling at the level of individual recycling events (Yudowski et al., 2006), we imaged MOR N-terminally tagged with a pH-sensitive GFP, SpH-MOR (Miesenböck et al., 1998). When expressed in HEK293 cells, MOR fluorescence was quenched in acidic endosomal compartments and dequenched upon recycling (Yudowski et al., 2009). Rapid imaging (10 Hz) using total internal reflection fluorescence (TIRF) microscopy (Puthenveedu et al., 2010; Yu et al., 2010) after MOR endocytosis revealed individual exocytic events as transient bursts of fluorescence at the cell surface (Figure 2A; Movie S1). The fluorescence burst showed a localized peak of maximum intensity that diffused across a larger area as vesicles fused and receptors diffused across the cell surface (Figures 2B [heat map at bottom] and 2C; Movie S2), consistent with our previous data that these are individual recycling events (Puthenveedu et al., 2010; Yudowski et al., 2009).

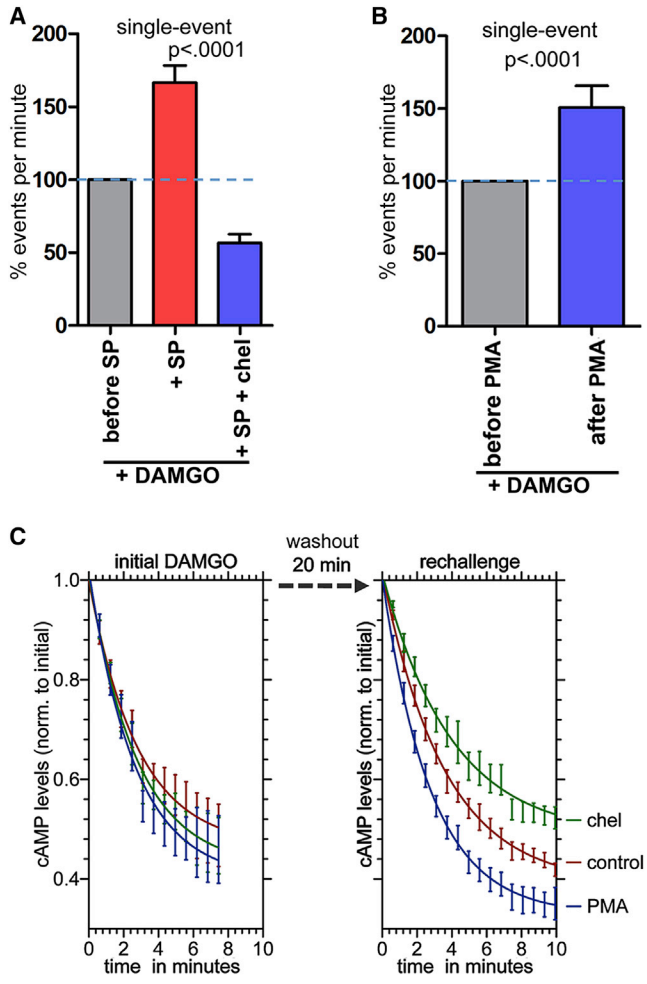

Figure 3. PKC Activation Is Required and Sufficient for SP-Induced Increase in MOR Recycling

(A) Percentage change in number of MOR recycling events, comparing SP to SP + chel. Chel blocked the SP-mediated increase. DG and either SP or SP + chel were added sequentially, and a paired comparison was made in the same cell (n = 12).

(B) PMA was sufficient to increase MOR recycling (n = 47 cells).

(C) Assay to detect resensitization of cells to MOR signaling using luminescence-based real-time detection of cAMP levels. The addition of DG reduces cAMP levels (left). Following DG washout (+ chel or PMA) to allow recycling, cells were rechallenged with DG. Chel (green) reduced recycling of functional MOR, while PMA (blue) enhanced it compared to control cells (red). The initial DG challenge was identical across all experiments. Error bars are SEM across nine experiments. See also Figure S2.

All error bars are ±SEM.

We calculated the percentage change in the number of recycling events after SP by normalizing to the initial rate before SP (Figure 2D). In cells expressing HA-NK1R, the percentage of MOR recycling events per minute increased after SP (Figures 2E and 2F; Movie S3), consistent with the increase we saw with endogenous NK1R (Figures 1C and 1E). In adjacent cells not expressing HA-NK1R, SP did not increase SpH-MOR recycling (Figure 2F). As HEK293 cells do not express noticeable levels of endogenous NK1R, this indicates that NK1R signaling is sufficient to increase MOR recycling. MOR recycling was not reduced by cycloheximide treatment, confirming that these were post-endocytic recycling events and not the insertion of newly synthesized protein (Figure S1A). Additionally, very few MOR recycling events were seen without DG stimulation, and SP did not change this (Figure S1B). Together, our results show that SP signaling increases MOR recycling through activation of the NK1R.

Protein Kinase C Signaling Is Required and Sufficient for SP-Induced Increase in MOR Recycling and Resensitization

We next addressed the intracellular NK1R signaling cascade that mediated the regulation of MOR recycling. NK1R couples to Gq/11, which activates protein kinase C (PKC) (Macdonald et al., 1996). The PKC inhibitor chelerythrine (chel) abolished the SP-induced increase in MOR recycling in NK1R-expressing cells (Figure 3A), indicating that PKC was required for SP- and NK1R-mediated regulation of MOR recycling. Additionally, PKC activation by Phorbol 12-myristate 13-acetate (PMA) increased SpH-MOR recycling in the absence of NK1R and SP (Figure 3B), indicating that PKC was sufficient for increasing MOR recycling. The addition of chel or PMA alone had no effect on SpH-MOR exocytic events (Figures S2A and S2B).

To investigate the functional consequences of PKC-mediated regulation of MOR recycling, we first measured DG-mediated inhibition of cyclic AMP (cAMP) levels as a readout of the number of functional surface MOR (Talbot et al., 2005). HEK293 cells expressing MOR were stimulated with DG for 15 min to induce MOR endocytosis and cellular desensitization. DG was washed out to allow MOR recycling, and cAMP inhibition in response to a rechallenge with DG was measured as an index of cellular resensitization. The addition of chel during the washout decreased cAMP inhibition after the rechallenge (Figure 3C, green line) compared to the control (Figure 3C, red line). In contrast, PMA increased cAMP inhibition in response to the DG rechallenge (Figure 3C, blue line). Chel and PMA alone, with no prior DG stimulation, had no effect on DG-induced inhibition of cAMP production (Figure S2C).

We next tested if PKC inhibition abolishes the SP-induced increase in MOR recycling in TG neurons, using the ratiometric recycling assay (Figure 1). The addition of chel during the washout abolished the SP-mediated increase in MOR recycling (Figures 4A and 4B). Pixel-based colocalization was lower when PKC was inhibited in the washout, even in the presence of SP (Figure 4C). Adding PMA without SP during the washout increased MOR recycling (Figures 4D and 4F). Together, this suggests that PKC is both required and sufficient for the regulation of MOR recycling and cellular sensitivity to opioid signaling.

SP- and PKC-Mediated Regulation of MOR Recycling Requires MOR Phosphorylation at Ser 363 and Thr 370

Considering that PKC was required and sufficient for heterologous regulation of MOR recycling through SP, we sought to identify the target of PKC. The MOR itself presented an interesting candidate. PKC can phosphorylate three sites on the C-terminal tail of MOR: serine 363, threonine 370, and serine 375 (Figure 5A; Doll et al., 2011; Feng et al., 2011). To test whether MOR

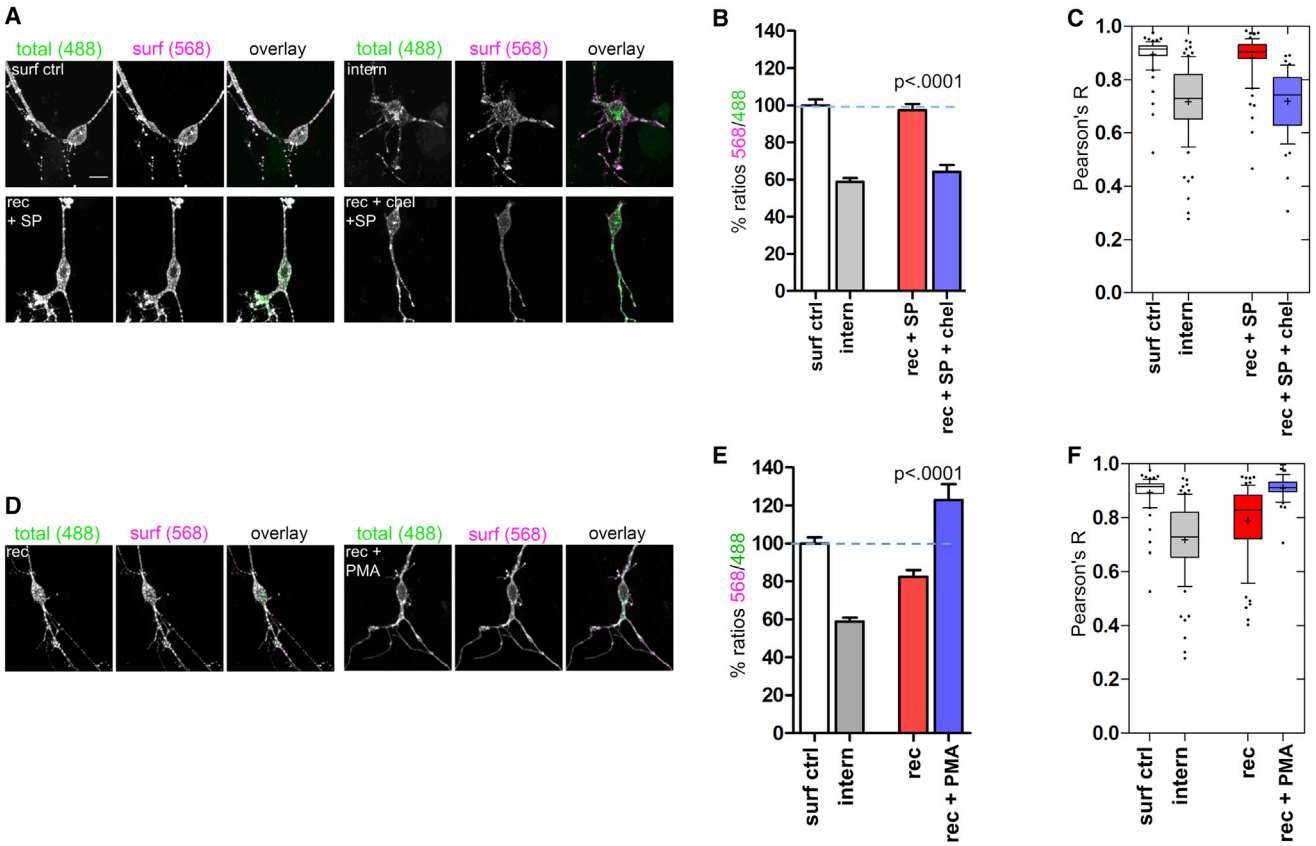

Figure 4. PKC Activation Is Required and Sufficient for SP-Induced Increase in MOR Recycling in TG Neurons

(A) Ratiometric recycling assay in TG neurons comparing MOR recycling in the presence of SP alone versus SP with chel. Scale bar represents 10 μm.

(B) Quantitation across multiple cells as in Figure 1C (mean ± SEM; n = 77 surf ctrl, 78 intern, 72 rec + SP, 47 rec + SP + chel).

(C) Tukey box plots of Pearson's coefficients from cells in (B).

(D and E) Ratiometric recycling assay in TG neurons testing the effect of PKC activation by PMA in the absence of SP (n = 77 surf ctrl, 78 intern, 69 rec, 47 rec + PMA).

(F) Tukey box plots of Pearson's coefficients from cells in (E).

All error bars are ±SEM.

phosphorylation was required, we mutated each of these sites to alanine to block phosphorylation (Feng et al., 2011) and quantified SP-mediated regulation of MOR recycling. SP did not increase the percentage of recycling events per unit time when either S363 or T370 was mutated (Figures 5B and 5C). In contrast, the recycling of S375A increased to a level comparable to wild-type in response to SP (Figures 5B and 5C). This indicates that S363 and T370 are required for SP-mediated regulation, but S375 is not (Figures 5B and 5C). Additionally, PMA increased SpH-MOR exocytic events for S375A, but not S363A or T370A, comparable to wild-type MOR (Figure 5D). In TG neurons, SP failed to increase S363A or T370A recycling (Figures 5E–5G for S363A and Figures 5H–5J for T370A), indicating that both S363 and T370 are required for PKC to regulate MOR recycling.

PKC Enhances Recycling and Resensitization of Endogenous MORs in TG Neurons

We next asked if endogenous MOR trafficking was regulated by PKC. To test this, we utilized a rabbit monoclonal anti-MOR antibody (UMB-3) to detect the subcellular localization of endogenous MORs (Lupp et al., 2011). UMB-3 staining showed strong staining at the periphery of TG neurons (Figure 6A), further indicated by the surface plot of intensity (Figure 6A, insets). To quantitate intracellular versus membrane MOR levels, UMB-3 fluorescence was measured across concentric circles increasing in size from the center to the periphery of the cell (Figure 6B). At steady state, the majority of UMB-3 maximum fluorescence intensity was detected in larger circles, consistent with more MOR localized to the surface (Figure 6B). After DG addition, UMB-3 staining was visible in punctate structures, and fluorescence intensity was uniform across the cell (Figures 6A and 6B), suggesting redistribution of MOR to endosomes. DG washout restored UMB-3 staining at the periphery of TG neurons (Figures 6A and 6B), consistent with MOR recycling. PKC inhibition during the washout inhibited MOR recycling, as evidenced by the retention of UMB-3 fluorescence in punctate structures and uniform fluorescence in smaller circles (Figures 6A and 6B). Conversely, PKC activation during the washout caused strong UMB-3 staining at the cell periphery (Figures 6A and 6B), suggesting that PKC increases endogenous MOR recycling.

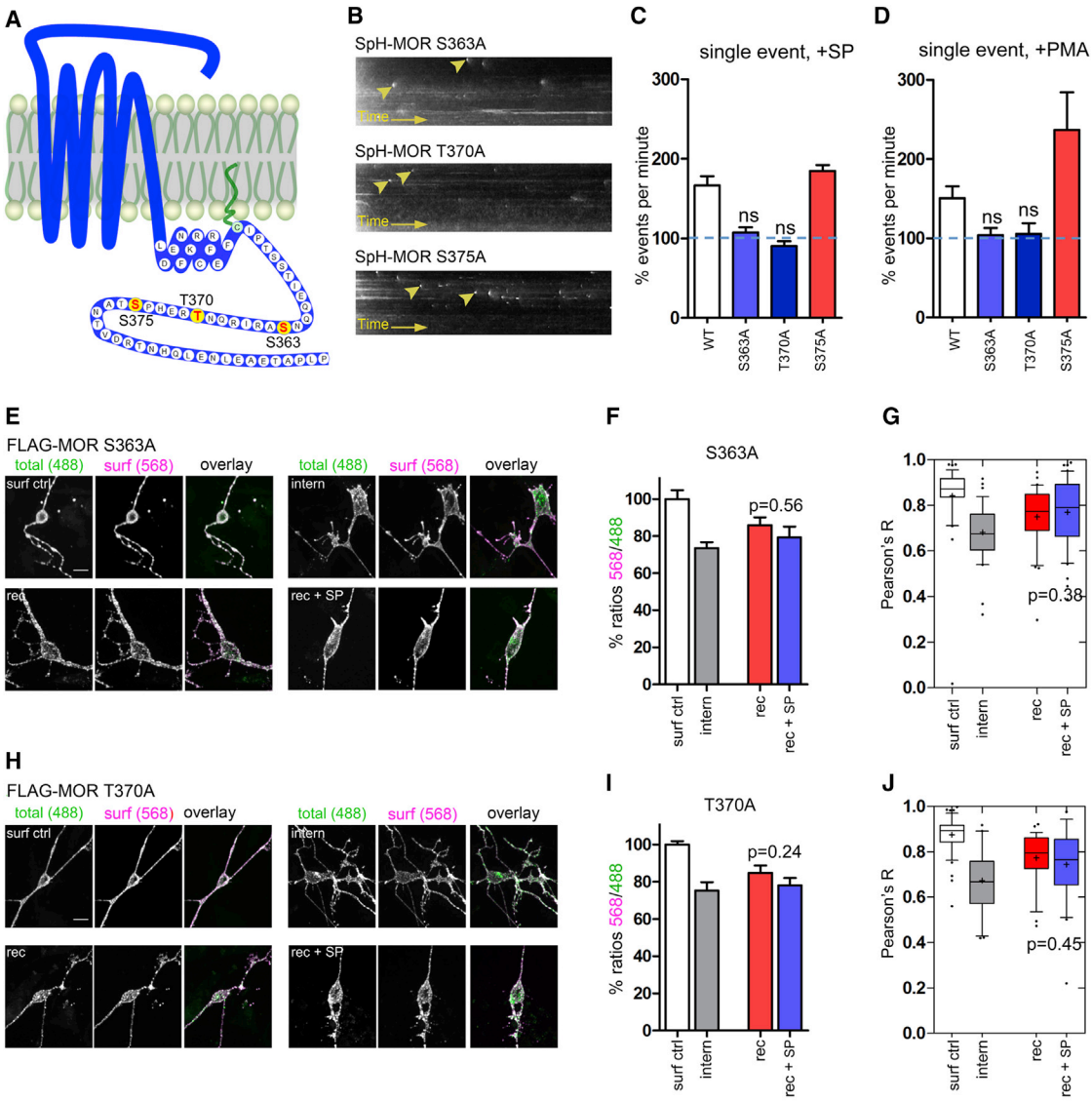

Figure 5. PKC Requires S363 and T370 to Regulate MOR Recycling

(A) Schematic of PKC phosphorylation sites on C-terminal tail of MOR (S363, T370, and S375).

(B) Kymographs of SpH-MOR single exocytic events for MOR S363A, T370A, and S375A after SP.

(C) Quantitation of percentage recycling across cells (n = 20, 14, 18, and 22) in HA-NK1R-expressing cells with MOR mutants S363A and T370A, and S375, compared to wild-type. Dashed line shows number of events in same cells prior to SP normalized to 100%.

(D) Percentage recycling with PMA-treated cells expressing MOR mutants S363A, T370A, and S375A (n = 52, 29, 18, and 17).

(E) Ratiometric recycling assay in TG neurons for S363A with and without SP. Scale bar represents 10 μm.

(F) Ratio quantitation across multiple cells (mean ± SEM; n = 35 surf ctrl, 38 intern, 33 rec, 41 rec + SP) between the washout without and with SP for S363A.

(G) Tukey box plots of Pearson's coefficients from S363A cells in (F) show no increase in correlation with SP.

(H) Ratiometric recycling assay in TG neurons for T370A with and without SP.

(I) Ratio quantitation (n = 47, 27, 29, and 27) without and with SP for T370A.

(J) Tukey box plots of Pearson's coefficients from T370A cells in (I) show no increase in correlation with SP. Scale bars represent 5 μm.

All error bars are ±SEM.

To further test PKC's regulation of endogenous MOR recycling in TG neurons, we used a fluorescent ligand, Alexa 594-conjugated dermorphin (derm594), previously described to bind MORs (Arttamangkul et al., 2000). To induce recycling, we treated TG neurons with DG, followed by a washout as in the re-sensitization experiment in Figure 3C. At the end, the cells were labeled with ice-cold derm594 to detect surface MOR. When compared to the control, DG significantly decreased derm594 fluorescence, consistent with MOR endocytosis. After washout, derm594 fluorescence was higher than the DG control,

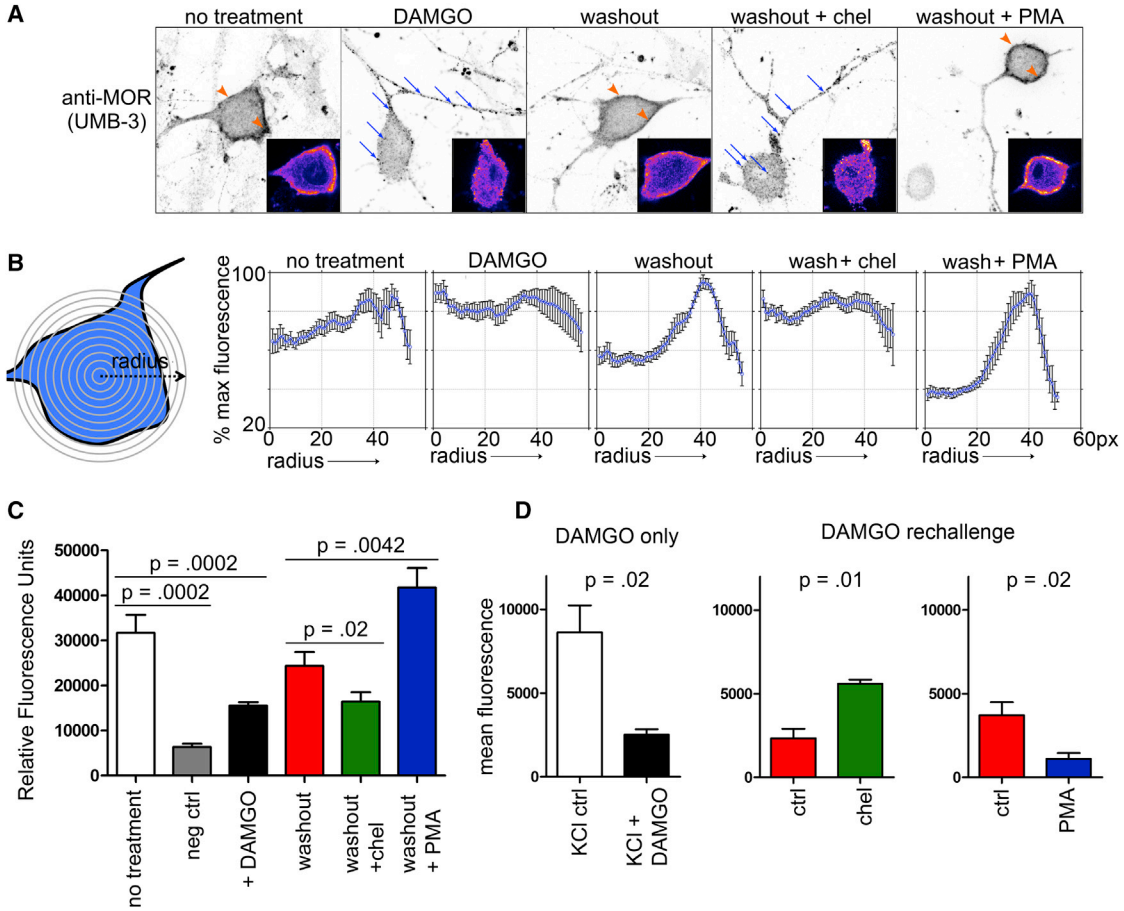

Figure 6. PKC Increases Recycling of Endogenous MOR and Opioid Resensitization in TG Neurons

(A) Example images of anti-MOR (UMB-3) in TG neurons. UMB-3 staining was primarily localized to the periphery in untreated cells (orange arrowheads). DG addition for 20 min induced a redistribution of UMB-3 staining to intracellular punctate structures (blue arrows). DG washout (20 min) induced greater UMB-3 staining at the periphery, similar to the untreated control. Addition of chel during the washout shifted UMB-3 staining to punctate structures, while PMA addition enhanced staining at the cell periphery. Insets show surface plots as heat maps.

(B) Schematic of radial profile method used to analyze fluorescence intensity of UMB-3 staining from the center to the periphery of cells. Intensity traces from multiple cells (mean ± SEM; n > 8 in each condition) show increased UMB-3 fluorescence in circles of larger radii, consistent with increased MOR on the surface. Higher fluorescence in larger radii denotes surface, while uniform fluorescence denotes internal pools.

(C) Graph of average mean intensity of derm-A594 signal labeling endogenous MOR in TG neurons across three trials (mean ± SEM) Derm-A594 fluorescence was significantly greater in non-treated TGs (no treatment) than HEK cells (neg ctrl), indicating specific binding. DG induced internalization, as shown by lower fluorescence (black bars). Washout increased fluorescence (red). Chel blocked this increase in fluorescence (green) and PMA enhanced it (blue).

(D) Graphs of mean fluorescence values of $DiBAC_4(5)$ in TG neurons, at 15 min after DG addition and DG rechallenge after the washout alone (left), with chel (center), and with PMA (right). Corresponding p values (mean ± SEM; n > 5 in each condition) are shown for each.

All error bars are ±SEM.

as expected after MOR recycling. PKC inhibition decreased derm594 fluorescence, and PKC activation increased it, suggesting that PKC increases recycling of endogenous MOR (Figure 6C). HEK293 cells not expressing MOR did not show fluorescence, confirming specificity of derm594 binding (Figure 6C). Together, these results suggest that PKC is required and sufficient to regulate recycling of endogenous MORs.

SP and PKC Regulate the Opioid Resensitization in Neurons and Opioid Analgesia in Mice

We next asked if PKC regulated the resensitization of opioid activity in physiologically relevant sensory neurons. TG neurons were incubated with the sulfonyl voltage-sensitive anionic dye $DiBAC_4(5)$ (George et al., 1988), which increases fluorescence on depolarization and decreases fluorescence on hyperpolarization. DG decreased the fluorescence of KCl-activated TG neurons, consistent with opioid-induced hyperpolarization (Figure 6D). To measure MOR recycling and resensitization, we used the agonist-washout paradigm above (Figures 6A–6C). After the initial DG challenge, DG was washed out for 20 min to allow recycling and resensitization. A rechallenge with DG decreased the KCl-induced voltage change similarly to the initial challenge, indicating that neurons were resensitized to opioid signaling (Figure 6D, left). However, when PKC was inhibited

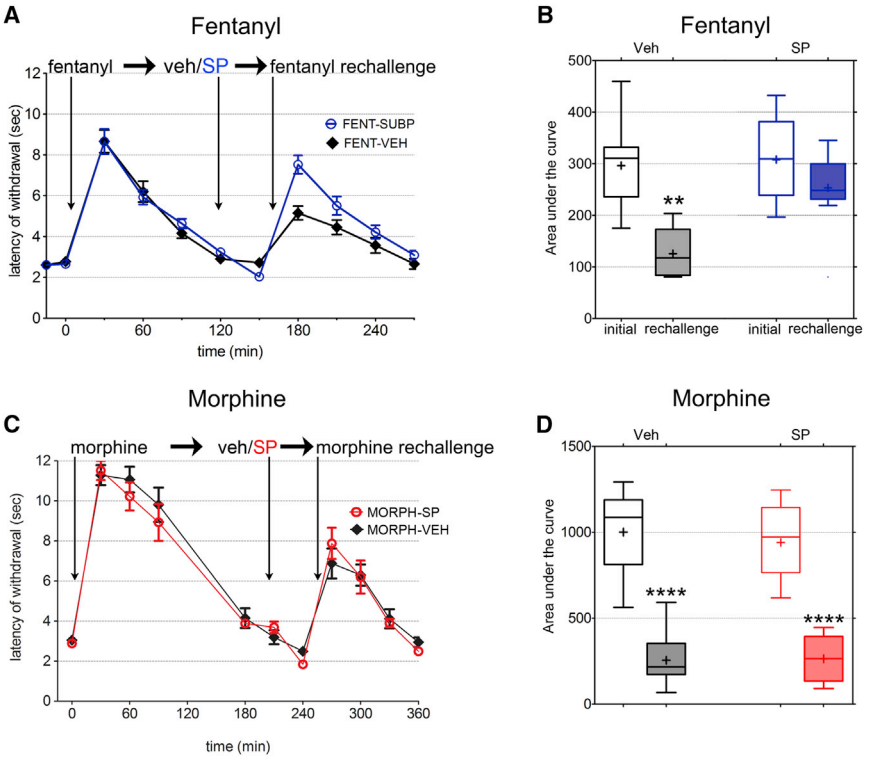

Figure 7. SP Reduces Acute Tolerance to Fentanyl, but Not Morphine

(A) Time course of fentanyl-induced antinociceptive responses. An increase in tail-withdrawal latencies denotes antinociception. The response after the second fentanyl injection is higher in SP-injected mice. Results are mean ± SEM (n = 9).

(B) Graph of areas under the curve for initial response and rechallenge for each condition.

(C) Time course of morphine-induced antinociceptive responses. Unlike fentanyl, the second morphine injection resulted in a lower response for both the vehicle control and SP-injected mice (mean ± SEM; n = 10 and 11).

(D) Graph of areas under the curve as in (B). See also Figure S3.

All error bars are ±SEM.

during the DG washout, the DG rechallenge did not decrease fluorescence, consistent with fewer receptors recycling back to the surface (Figure 6D, middle). Further, PKC activation during the DG washout enhanced the effect of the DG rechallenge (Figure 6D, right). This suggests that PKC regulates opioid resensitization in sensory neurons, consistent with our model that SP-mediated PKC activation positively regulates MOR recycling and resensitization.

To test if SP regulated the resensitization of MOR-mediated analgesia in mice, we measured the development of acute tolerance to the antinociceptive effects of fentanyl, a short-acting MOR agonist, using a warm-water tail-withdrawal assay (Melief et al., 2010; Pradhan et al., 2010; Figure S3A). After baseline measurements, animals were injected with fentanyl, and tail-withdrawal latencies were measured every 30 min. A significant but sub-maximal increase in tail-withdrawal latencies, persisting for approximately 120 min, was observed with fentanyl (Figure 7A). Either saline (vehicle control) or SP was injected intrathecally 120 min after the first fentanyl challenge. In control mice, a fentanyl rechallenge, given 30 min later, attenuated (~40% of initial) the antinociceptive response, indicating acute tolerance to fentanyl (Figure 7A). In contrast, SP-injected mice showed an antinociceptive response to the rechallenge that was comparable to the initial response (Figures 7A and S3B). Calculation of the areas under the curve showed that saline-injected mice showed a significantly reduced response to the fentanyl rechallenge compared to the initial response, while SP-injected mice showed comparable responses to both fentanyl injections (Figure 7B). Because morphine-activated MORs were not subject to SP-regulated recycling, we next tested if SP could sensitize morphine-induced analgesia in mice. Consistent with our cellular data, a morphine rechallenge following SP injection did not increase tail-withdrawal latency in contrast to fentanyl (Figures 7C and 7D and S3C). Taken together, our results indicate that SP signaling through PKC inhibits acute tolerance to fentanyl, but not morphine, by increasing MOR recycling in peripheral neurons.

DISCUSSION

We show that SP signaling, through endogenous NK1R, enhances MOR recycling following DG- and fentanyl-, but not morphine-induced endocytosis (Figures 1 and 2). PKC activity downstream of NK1R is required and sufficient for this crosstalk (Figures 3 and 4). We identify two PKC sites on the C-terminal tail of MOR as the targets for this NK1R-mediated regulation (Figure 5), and show a functional effect of PKC regulation in the recycling of exogenous and endogenous MOR in sensory neurons (Figure 6). Further, we show that SP increases opioid antinociception in mice by attenuating acute tolerance to fentanyl, but not morphine.

Studies over the last decades have suggested a complex and paradoxical interaction between the neurokinin and opioid pathways. SP, a pain-associated neurotransmitter, can induce antinociceptive effects (Mohrland and Gebhart, 1979). Further, NK1R antagonists can modify opioid reward, withdrawal, and reinforcement, and NK1R is required for morphine reward but not morphine analgesia (Gadd et al., 2003; Murtra et al., 2000). Our data, that SP regulates MOR recycling and acute tolerance to fentanyl, but not morphine (Figure 7), are consistent with this, but suggest a complex agonist-selective crosstalk between these pathways. At a cellular level, co-activation of NK1R and MOR in CNS neurons has been reported to inhibit MOR endocytosis, partly because NK1R non-specifically sequesters beta-arrestin, the common adaptor required for GPCR endocytosis

(Pierce et al., 2002; Yu et al., 2009), and partly because the receptors might heterodimerize (Pfeiffer et al., 2003). We directly measured individual recycling events, which allowed us to test acute regulation of MOR recycling induced by NK1R signaling in the same cell (Figure 2), free of the potentially confounding effect of NK1R on MOR endocytosis. Further, in our ratiometric assay, NK1Rs were activated after MOR was endocytosed, and the presence of a MOR antagonist prevented subsequent endocytosis. Therefore, we believe endocytosis has a negligible effect on the crosstalk we observed here. Further, blocking new MOR synthesis (Figure S1) had no effect on the surface delivery of MOR in our assays, and inhibition or activation of PKC without DG did not cause any change in MOR surface levels or induce surface insertion (Figure S2). Therefore, the increase in surface MOR we observed was primarily a result of increased recycling (Figures 1 and 2).

The precise role of PKC in modulating opioid physiology and MOR trafficking is unresolved (Raehal et al., 2011; Williams et al., 2013), but it provides a potential control point for physiological regulation of opioid signaling. PKC has been implicated in controlling opiate resensitization, tolerance, and dependence, and PKC activation during prolonged MOR agonist exposure increases desensitization, possibly by endocytosis (Dang and Williams, 2004; Inoue and Ueda, 2000; Bailey et al., 2004; Kramer and Simon, 1999). Given that MOR itself can activate PKC, such homologous PKC activation during chronic MOR activation might regulate desensitization and endocytosis, whereas injury and inflammatory pain might alter the balance of MOR trafficking and resensitization through heterologous SP regulation, consistent with data that peripheral MORs are less active prior to injury or pain (Berg et al., 2007; Chen and Marvizón, 2009).

Such distinct cell-type or environment-dependent consequences could be brought about by differential MOR phosphorylation. Because we added SP after the major fraction of MOR already was internalized, we believe that the endosomal pool of MOR can be phosphorylated by PKC. Of the two MOR PKC targets required for SP-mediated increase in MOR recycling, S363 was constitutively phosphorylated, while T370 phosphorylation was regulated. Interestingly, T370 was phosphorylated by DG, but not morphine (Doll et al., 2011). However, it was robustly phosphorylated by heterologous SP and PKC activity (Illing et al., 2014; Mann et al., 2015), so it is unlikely to be the primary explanation for the differences we saw between DG and morphine. S375 might be phosphorylated primarily by GPCR kinases (GRK) rather than PKC (Doll et al., 2012), consistent with our result that S375 was not required for NK1R's regulation of MOR recycling via PKC. Additionally, T370 might be phosphorylated by GRK 2/3 following MOR activation with a hierarchical dependence on S375 phosphorylation (Just et al., 2013), and inhibition of GRK2 alleviates opiate tolerance (Dang et al., 2011). Further, SP induced PKC-dependent phosphorylation of MOR at T370 without dependence on S375 phosphorylation (Illing et al., 2014). It is possible that T370 is differentially phosphorylated by PKCs and GRKs by homologous versus heterologous regulation to control physiological consequences in different cell types. Homologous GRK-mediated phosphorylation of MOR following the addition of opioid agonists might promote opioid tolerance in the CNS, while PKC phosphorylation at T370 following NK1R activation induces resensitization of MORs in the context of inflammatory pain in the peripheral nervous system (PNS).

T370 and S363 are adjacent to a bi-leucine sequence that is required and sufficient for MOR recycling (Tanowitz and von Zastrow, 2003). This raises the possibility that combinatorial MOR phosphorylation by homologous and heterologous signaling pathways might rapidly reprogram receptor recycling and cellular resensitization by changing the biochemical interactions of MOR. Reprogramming in response to homologous regulation has been suggested for B2AR recycling, which switches between a sequence-dependent and bulk recycling pathway based on PKA phosphorylation (Puthenveedu et al., 2010; Vistein and Puthenveedu, 2013). MOR recycling in striatal neurons has been reported to be inhibited by forskolin, though PKA was not directly tested (Roman-Vendrell et al., 2012). Striatal neurons do not co-express NK1R and MOR, and it is possible that different neuronal subtypes exhibit distinct mechanisms of regulation, depending on the expression profiles of signaling receptors and kinases. Rapid reprogramming by receptor phosphorylation could therefore be a general mechanism to switch receptors between different recycling pathways, depending on the physiological circumstance. For MOR, such reprogramming, causing sensitization of nociceptors to opioid signaling, could in part explain the paradoxical analgesic effects of capsaicin and SP (Komatsu et al., 2009; Mohrland and Gebhart, 1979). We show that peripheral administration of SP is capable of increasing MOR-mediated analgesia in mice. This is consistent with data that peripheral endogenous opioids are released following tissue damage and painful stimuli, and that this is accompanied by an increase in opioid receptors to nerve terminals (Stein and Lang, 2009). As the opioid system serves as a physiological check for the maladaptive consequences of pain, our results provide a proof of principle for how signaling crosstalk between these systems at the level of receptor trafficking could represent a general homeostatic mechanism of signaling crosstalk.

EXPERIMENTAL PROCEDURES

Plasmid DNA and Constructs

FLAG-MOR and SpH-MOR have been described previously (Keith et al., 1996; Soohoo and Puthenveedu, 2013). HA-tagged rat NK1R was provided by Dr. Mark von Zastrow. Point mutants were generated using site-directed mutagenesis with QuikChange (Agilent Technologies). All constructs were confirmed by DNA sequencing.

Cell Cultures and Transfections

TG neurons were obtained as previously described (Malin et al., 2007), and transfected using Lipofectamine 2000 (Invitrogen) 2 days after plating. Cells were maintained for 2 days in culture before imaging. HEK293 cells were obtained from ATCC and maintained in DMEM (Fisher Scientific) + 10% fetal bovine serum (FBS). Cells were transfected with Effectene (QIAGEN). Stable cell lines were generated with Geneticin (Invitrogen) selection. Cells were passed to 25 mm coverglass 1 day after transfection and imaged the following day.

Immunofluorescence Ratiometric Recycling Assay and Quantification

TGs expressing FLAG-MOR were labeled with Alexa 488-conjugated M1 anti-FLAG to label surface receptors for 10 min, followed by incubation with 10 μM

DG (Sigma-Aldrich) for 20 min to promote receptor internalization. Agonist media were washed out and replaced with media containing 10 μM naltrexone (Sigma), a MOR antagonist, to prevent additional activation and internalization of MOR for 20 min. Recycled surface M1-anti-FLAG-labeled receptors were then labeled with secondary goat anti-mouse conjugated to Alexa 568 for 10 min at 4°C. All other incubations were performed at 37°C. Cells were then fixed with 4% paraformaldehyde (PFA) for 20 min, and blocked with 0.1 M glycine in complete PBS for 10 min.

A surface control was performed, where cells were labeled for 10 min with Alexa 488-M1 anti-FLAG, immediately followed by Alexa 568-secondary goat anti-mouse to quantify the steady-state amount of surface receptors. An endocytosis control was performed, where cells were labeled with the secondary antibody and fixed, to quantify the amount of receptors internalized in the presence of DG. The percentage recycling was calculated from the ratio of intensities of the secondary antibody to the primary anti-FLAG and by dividing experimental conditions by the surface control minus the endocytosis control (expt condition − endo ctrl)/(surf ctrl − endo ctrl)%. Just Another Colocalization Plugin (JACoP) for ImageJ was used to generate a cytofluorogram and Pearson's correlation coefficient of intensities between primary and secondary antibody fluorescence. Statistical analyses and graphing were done using Microsoft Excel and GraphPad Prism. p values are from Mann-Whitney tests.

Individual Exocytic Event Recycling Assay

HEK293 cells stably expressing SpH-MOR were incubated in DG for 5 min, and a 1-min movie was acquired at 10 Hz using TIRF microscopy, followed by subsequent incubation with the second drug and a 1-min movie, at 37°C. For SP experiments, cells were transiently transfected with HA-NK1R. Cells were incubated in anti-HA (Sigma-Aldrich), followed by Alexa 568-goat anti-mouse, both for 10 min. Cells were incubated for 5 min with DG, and a 1-min movie was acquired. SP was added for 5 min, followed by a 1-min movie. Individual insertion events were manually counted using a double-blind process. A paired comparison was made within the same cell, normalizing to the agonist-only treatment. Significance was determined through Student's paired t test.

Live Cell and Fluorescence Imaging

Cells were imaged using a Nikon TE-2000E inverted microscope with a 60× 1.49 NA TIRF objective, Andor Revolution XD spinning disk confocal system, and 488 and 568 nm solid-state lasers. Cells were imaged in Opti-MEM or Leibowitz's L15 medium (Gibco), 5% FBS, at 37°C. Time lapses were acquired using an Andor iXon+ EM-CCD camera using Andor IQ. Original 16-bit tif files acquired directly from the camera were used for image analysis.

Fluorescent Ligand Binding

TG neurons were plated on a clear-bottom black 96-well plate for 2 days. Cells were stimulated with DG for 15 min to induce internalization, followed by a 15-min DG washout with naltrexone to induce MOR recycling, at 37°C. Two parallel controls, no DG or naltrexone treatment and a DG-only treatment, were performed. Cells were washed and labeled with 100 nM derm594 (in cold PBS, Ca/Mg) at room temperature, then washed out two times. Fluorescence was recorded on a Tecan Safire II Plate Reader at (at 25°C). Derm594 was generously donated by Dr. John Williams (Vollum Institute).

UMB-3 Immunofluorescence Staining

TG neurons, plated on coverglass, were treated either with DG (endo ctrl), no drug (surf ctrl), or incubated with DG for 20 min, followed by agonist washout with antagonist and vehicle, chel, or PMA for 20 min (recycling). Cells were then fixed in 4% PFA for 25 min, blocked, and permeabilized in PBS + Ca/Mg, FBS, and 0.01% Triton for 45 min. Cells were incubated with UMB-3 in PBS + Ca/Mg at 4°C overnight, and labeled with Alexa 488-goat anti-rabbit secondary antibody, mounted, and imaged.

cAMP Measurement

Assays were performed on HEK293 cells stably expressing MOR and cAMP-Glo Sensor 20F (Promega), at 35°C with IBMX. Luminescence was continuously recorded using a Tecan Infinite M1000 Plate Reader. After 5 min of baseline, DG was added for 10 min to record the initial response and allow endocytosis; media were washed out and replaced with media with naltrexone and either PMA, chel, or vehicle for 20 min for recycling. A rechallenge with DG was used to measure resensitization of recycled MORs.

Voltage-Sensitive Dye Measurement

For control KCl and DG experiments, TG neurons were labeled with $DiBAC_4(5)$ and imaged every 30 s. Then 80 mM KCl was added to depolarize TGs, and DG was added 5 min after KCl to activate endogenous MORs. Cells were incubated with 10 μM DG for 15 min. The agonist was washed out and replaced with media and 10 μM naltrexone and PMA or chel, and compared to naltrexone-only washout. The antagonist was washed out, for 20 min (chel) or 10 min (PMA), and cells were labeled with $DiBAC_4(5)$. Cells were rechallenged 5 m after KCl with 10 μM DG and imaged. Mean fluorescence was analyzed using ImageJ, and statistical analyses and graphing were performed in GraphPad Prism.

Tail Immersion Assay

Subjects were male C57BL6/J mice between 9 and 12 weeks old. Animals were group housed in a 14 hr/10 hr light/dark cycle, and food and water were available ad libitum. All experiments were in accordance with the Association for Assessment and Accreditation of Laboratory Animal Care International (AALAC) guidelines and were approved by the Animal Care Committee at the University of Illinois, Chicago. Thermal nociception was determined using the warm-water tail-withdrawal assay. Animals were initially habituated to the test apparatus for 2 days before testing. On the test day, mice were lightly restrained in a conical restraint bag, and their tails were immersed (5 cm from the tip) into a 52.5°C water bath. Tail-withdrawal latencies were determined, and a cutoff of 12 s was established. After three basal measurements, mice were injected with fentanyl (0.1 mg/kg, subcutaneously [SC]) or morphine (5 mg/kg, SC), and tested every 30 min for 4.5 to 6 hr (Melief et al., 2010). At 120 min (fentanyl) or 210 min (morphine), mice were injected intrathecally with 5 μl SP (10 ng) or 0.9% saline. Intrathecal injections were performed with a 30-gauge, 1/2-inch needle at the L4–5 lumbar interspace on lightly anesthetized mice. Tail twitch was used to confirm needle placement, and any mice that exhibited motor impairment following intrathecal injection were excluded. Mice were injected 30 min later with a second injection of fentanyl (0.1 mg/kg, SC) or morphine (5 mg/kg, SC), and tested every 30 min until tail-withdrawal latencies returned back to baseline responses.

SUPPLEMENTAL INFORMATION

Supplemental Information includes three figures and three movies and can be found with this article online at http://dx.doi.org/10.1016/j.celrep.2015.02.045.

AUTHOR CONTRIBUTIONS

S.L.B., A.L.S., and M.A.P. conceived the project and designed experiments. S.L.B. performed two-color ratiometric recycling assays in TG neurons, live-cell SpH-MOR imaging experiments in HEK293 cells, live-cell experiments with voltage-sensing dye and derm594, and immunofluorescence experiments with UMB-3 anti-MOR. A.L.S. performed live-cell SpH-MOR imaging experiments in HEK293 cells and site-directed mutagenesis of SpH-MOR S363-T370A. D.J.S. performed experiments with Promega cAMP luminescence sensor. A.A.P. performed antinociception assays in mice. S.S. developed and provided UMB-3 anti-MOR. S.L.B., A.L.S., D.J.S., A.A.P., and M.A.P. analyzed and interpreted data. S.L.B., A.L.S., and M.A.P. wrote this manuscript, which was reviewed by all authors.

ACKNOWLEDGMENTS

We thank Dr. Alison Barth, Joanne Steinmiller, Jen Dry-Henich, Dr. Rebecca Seal, and Adam Goldring for providing help with isolation of TG neurons and for critical comments. We thank Drs. Mark von Zastrow and Rachel Vistein for reagents and technical help. We thank Drs. John T. Williams and Seksiri Arttamangkul for generously providing the Alexa 594-conjugated dermorphin. We thank Drs. Adam Linstedt, Tina Lee, Joann Trejo, Peter Friedman, Guillermo

Romero, Jean-Pierre Vilardaga, Alessandro Bisello, and Aylin Hanyaloglu for comments and suggestions. S.L.B. was supported by an NIH T32 grant NS007433, A.A.P. was supported by NIH DA031243, and M.A.P. was supported by NIH DA024698 and DA036086.

Received: April 27, 2014
Revised: October 31, 2014
Accepted: February 18, 2015
Published: March 19, 2015

REFERENCES

Aicher, S.A., Punnoose, A., and Goldberg, A. (2000). μ-Opioid receptors often colocalize with the substance P receptor (NK1) in the trigeminal dorsal horn. J. Neurosci. *20*, 4345–4354.

Alvarez, V.A., Arttamangkul, S., Dang, V., Salem, A., Whistler, J.L., Von Zastrow, M., Grandy, D.K., and Williams, J.T. (2002). mu-Opioid receptors: Ligand-dependent activation of potassium conductance, desensitization, and internalization. J. Neurosci. *22*, 5769–5776.

Anggono, V., and Huganir, R.L. (2012). Regulation of AMPA receptor trafficking and synaptic plasticity. Curr. Opin. Neurobiol. *22*, 461–469.

Arttamangkul, S., Alvarez-Maubecin, V., Thomas, G., Williams, J.T., and Grandy, D.K. (2000). Binding and internalization of fluorescent opioid peptide conjugates in living cells. Mol. Pharmacol. *58*, 1570–1580.

Arttamangkul, S., Quillinan, N., Low, M.J., von Zastrow, M., Pintar, J., and Williams, J.T. (2008). Differential activation and trafficking of micro-opioid receptors in brain slices. Mol. Pharmacol. *74*, 972–979.

Arttamangkul, S., Lau, E.K., Lu, H.W., and Williams, J.T. (2012). Desensitization and trafficking of μ-opioid receptors in locus ceruleus neurons: modulation by kinases. Mol. Pharmacol. *81*, 348–355.

Bailey, C.P., Kelly, E., and Henderson, G. (2004). Protein kinase C activation enhances morphine-induced rapid desensitization of μ-opioid receptors in mature rat locus ceruleus neurons. Mol. Pharmacol. *66*, 1592–1598.

Berg, K.A., Patwardhan, A.M., Sanchez, T.A., Silva, Y.M., Hargreaves, K.M., and Clarke, W.P. (2007). Rapid modulation of micro-opioid receptor signaling in primary sensory neurons. J. Pharmacol. Exp. Ther. *321*, 839–847.

Chen, W., and Marvizón, J.C.G. (2009). Acute inflammation induces segmental, bilateral, supraspinally mediated opioid release in the rat spinal cord, as measured by mu-opioid receptor internalization. Neuroscience *161*, 157–172.

Claing, A., Laporte, S.A., Caron, M.G., and Lefkowitz, R.J. (2002). Endocytosis of G protein-coupled receptors: roles of G protein-coupled receptor kinases and beta-arrestin proteins. Prog. Neurobiol. *66*, 61–79.

Dang, V.C., and Williams, J.T. (2004). Chronic morphine treatment reduces recovery from opioid desensitization. J. Neurosci. *24*, 7699–7706.

Dang, V.C., Chieng, B., Azriel, Y., and Christie, M.J. (2011). Cellular morphine tolerance produced by βarrestin-2-dependent impairment of μ-opioid receptor resensitization. J. Neurosci. *31*, 7122–7130.

De Felipe, C., Herrero, J.F., O'Brien, J.A., Palmer, J.A., Doyle, C.A., Smith, A.J., Laird, J.M., Belmonte, C., Cervero, F., and Hunt, S.P. (1998). Altered nociception, analgesia and aggression in mice lacking the receptor for substance P. Nature *392*, 394–397.

Doll, C., Konietzko, J., Pöll, F., Koch, T., Höllt, V., and Schulz, S. (2011). Agonist-selective patterns of μ-opioid receptor phosphorylation revealed by phosphosite-specific antibodies. Br. J. Pharmacol. *164*, 298–307.

Doll, C., Pöll, F., Peuker, K., Loktev, A., Glück, L., and Schulz, S. (2012). Deciphering μ-opioid receptor phosphorylation and dephosphorylation in HEK293 cells. Br. J. Pharmacol. *167*, 1259–1270.

Feng, B., Li, Z., and Wang, J.B. (2011). Protein kinase C-mediated phosphorylation of the μ-opioid receptor and its effects on receptor signaling. Mol. Pharmacol. *79*, 768–775.

Gadd, C.A., Murtra, P., De Felipe, C., and Hunt, S.P. (2003). Neurokinin-1 receptor-expressing neurons in the amygdala modulate morphine reward and anxiety behaviors in the mouse. J. Neurosci. *23*, 8271–8280.

Gainetdinov, R.R., Premont, R.T., Bohn, L.M., Lefkowitz, R.J., and Caron, M.G. (2004). Desensitization of G protein-coupled receptors and neuronal functions. Annu. Rev. Neurosci. *27*, 107–144.

George, E.B., Nyirjesy, P., Pratap, P.R., Freedman, J.C., and Waggoner, A.S. (1988). Impermeant potential-sensitive oxonol dyes: III. The dependence of the absorption signal on membrane potential. J. Membr. Biol. *105*, 55–64.

Hanyaloglu, A.C., and von Zastrow, M. (2007). A novel sorting sequence in the beta2-adrenergic receptor switches recycling from default to the Hrs-dependent mechanism. J. Biol. Chem. *282*, 3095–3104.

Hunt, S.P., and Mantyh, P.W. (2001). The molecular dynamics of pain control. Nat. Rev. Neurosci. *2*, 83–91.

Illing, S., Mann, A., and Schulz, S. (2014). Heterologous regulation of agonist-independent μ-opioid receptor phosphorylation by protein kinase C. Br. J. Pharmacol. *171*, 1330–1340.

Inoue, M., and Ueda, H. (2000). Protein kinase C-mediated acute tolerance to peripheral mu-opioid analgesia in the bradykinin-nociception test in mice. J. Pharmacol. Exp. Ther. *293*, 662–669.

Jean-Alphonse, F., and Hanyaloglu, A.C. (2011). Regulation of GPCR signal networks via membrane trafficking. Mol. Cell. Endocrinol. *331*, 205–214.

Just, S., Illing, S., Trester-Zedlitz, M., Lau, E.K., Kotowski, S.J., Miess, E., Mann, A., Doll, C., Trinidad, J.C., Burlingame, A.L., et al. (2013). Differentiation of opioid drug effects by hierarchical multi-site phosphorylation. Mol. Pharmacol. *83*, 633–639.

Keith, D.E., Murray, S.R., Zaki, P.A., Chu, P.C., Lissin, D.V., Kang, L., Evans, C.J., and von Zastrow, M. (1996). Morphine activates opioid receptors without causing their rapid internalization. J. Biol. Chem. *271*, 19021–19024.

Kieffer, B.L. (1995). Recent advances in molecular recognition and signal transduction of active peptides: receptors for opioid peptides. Cell. Mol. Neurobiol. *15*, 615–635.

Komatsu, T., Sasaki, M., Sanai, K., Kuwahata, H., Sakurada, C., Tsuzuki, M., Iwata, Y., Sakurada, S., and Sakurada, T. (2009). Intrathecal substance P augments morphine-induced antinociception: possible relevance in the production of substance P N-terminal fragments. Peptides *30*, 1689–1696.

Kramer, H.K., and Simon, E.J. (1999). Role of protein kinase C (PKC) in agonist-induced mu-opioid receptor down-regulation: II. Activation and involvement of the alpha, epsilon, and zeta isoforms of PKC. J. Neurochem. *72*, 594–604.

Lao, L., Song, B., Chen, W., and Marvizón, J.C. (2008). Noxious mechanical stimulation evokes the segmental release of opioid peptides that induce μ-opioid receptor internalization in the presence of peptidase inhibitors. Brain Res. *1197*, 85–93.

Lupp, A., Richter, N., Doll, C., Nagel, F., and Schulz, S. (2011). UMB-3, a novel rabbit monoclonal antibody, for assessing μ-opioid receptor expression in mouse, rat and human formalin-fixed and paraffin-embedded tissues. Regul. Pept. *167*, 9–13.

Macdonald, S.G., Dumas, J.J., and Boyd, N.D. (1996). Chemical cross-linking of the substance P (NK-1) receptor to the α subunits of the G proteins Gq and G11. Biochemistry *35*, 2909–2916.

Malin, S.A., Davis, B.M., and Molliver, D.C. (2007). Production of dissociated sensory neuron cultures and considerations for their use in studying neuronal function and plasticity. Nat. Protoc. *2*, 152–160.

Mann, A., Illing, S., Miess, E., and Schulz, S. (2015). Different mechanisms of homologous and heterologous μ-opioid receptor phosphorylation. Br. J. Pharmacol. *172*, 311–316.

Marchese, A., Paing, M.M., Temple, B.R.S., and Trejo, J. (2008). G protein-coupled receptor sorting to endosomes and lysosomes. Annu. Rev. Pharmacol. Toxicol. *48*, 601–629.

Martini, L., and Whistler, J.L. (2007). The role of mu opioid receptor desensitization and endocytosis in morphine tolerance and dependence. Curr. Opin. Neurobiol. *17*, 556–564.

Melief, E.J., Miyatake, M., Bruchas, M.R., and Chavkin, C. (2010). Ligand-directed c-Jun N-terminal kinase activation disrupts opioid receptor signaling. Proc. Natl. Acad. Sci. USA *107*, 11608–11613.

Miesenböck, G., De Angelis, D.A., and Rothman, J.E. (1998). Visualizing secretion and synaptic transmission with pH-sensitive green fluorescent proteins. Nature *394*, 192–195.

Mohrland, J.S., and Gebhart, G.F. (1979). Substance P-induced analgesia in the rat. Brain Res. *171*, 556–559.

Murtra, P., Sheasby, A.M., Hunt, S.P., and De Felipe, C. (2000). Rewarding effects of opiates are absent in mice lacking the receptor for substance P. Nature *405*, 180–183.

Nichols, M.L., Allen, B.J., Rogers, S.D., Ghilardi, J.R., Honore, P., Luger, N.M., Finke, M.P., Li, J., Lappi, D.A., Simone, D.A., and Mantyh, P.W. (1999). Transmission of chronic nociception by spinal neurons expressing the substance P receptor. Science *286*, 1558–1561.

Perl, E.R. (2007). Ideas about pain, a historical view. Nat. Rev. Neurosci. *8*, 71–80.

Pfeiffer, M., Kirscht, S., Stumm, R., Koch, T., Wu, D., Laugsch, M., Schröder, H., Höllt, V., and Schulz, S. (2003). Heterodimerization of substance P and μ-opioid receptors regulates receptor trafficking and resensitization. J. Biol. Chem. *278*, 51630–51637.

Pierce, K.L., Premont, R.T., and Lefkowitz, R.J. (2002). Seven-transmembrane receptors. Nat. Rev. Mol. Cell Biol. *3*, 639–650.

Pradhan, A.A., Walwyn, W., Nozaki, C., Filliol, D., Erbs, E., Matifas, A., Evans, C., and Kieffer, B.L. (2010). Ligand-directed trafficking of the δ-opioid receptor in vivo: two paths toward analgesic tolerance. J. Neurosci. *30*, 16459–16468.

Premont, R.T., and Gainetdinov, R.R. (2007). Physiological roles of G protein-coupled receptor kinases and arrestins. Annu. Rev. Physiol. *69*, 511–534.

Puthenveedu, M.A., Lauffer, B., Temkin, P., Vistein, R., Carlton, P., Thorn, K., Taunton, J., Weiner, O.D., Parton, R.G., and von Zastrow, M. (2010). Sequence-dependent sorting of recycling proteins by actin-stabilized endosomal microdomains. Cell *143*, 761–773.

Raehal, K.M., Schmid, C.L., Groer, C.E., and Bohn, L.M. (2011). Functional selectivity at the μ-opioid receptor: implications for understanding opioid analgesia and tolerance. Pharmacol. Rev. *63*, 1001–1019.

Roman-Vendrell, C., Yu, Y.J., and Yudowski, G.A. (2012). Fast modulation of μ-opioid receptor (MOR) recycling is mediated by receptor agonists. J. Biol. Chem. *287*, 14782–14791.

Rosenbaum, D.M., Rasmussen, S.G.F., and Kobilka, B.K. (2009). The structure and function of G-protein-coupled receptors. Nature *459*, 356–363.

Scita, G., and Di Fiore, P.P. (2010). The endocytic matrix. Nature *463*, 464–473.

Shepherd, J.D., and Huganir, R.L. (2007). The cell biology of synaptic plasticity: AMPA receptor trafficking. Annu. Rev. Cell Dev. Biol. *23*, 613–643.

Soohoo, A.L., and Puthenveedu, M.A. (2013). Divergent modes for cargo-mediated control of clathrin-coated pit dynamics. Mol. Biol. Cell *24*, 1725–1734, S1–S12.

Sorkin, A., and von Zastrow, M. (2009). Endocytosis and signalling: intertwining molecular networks. Nat. Rev. Mol. Cell Biol. *10*, 609–622.

Stein, C., and Lang, L.J. (2009). Peripheral mechanisms of opioid analgesia. Curr. Opin. Pharmacol. *9*, 3–8.

Talbot, J.N., Happe, H.K., and Murrin, L.C. (2005). Mu opioid receptor coupling to Gi/o proteins increases during postnatal development in rat brain. J. Pharmacol. Exp. Ther. *314*, 596–602.

Tanowitz, M., and von Zastrow, M. (2003). A novel endocytic recycling signal that distinguishes the membrane trafficking of naturally occurring opioid receptors. J. Biol. Chem. *278*, 45978–45986.

Vistein, R., and Puthenveedu, M.A. (2013). Reprogramming of G protein-coupled receptor recycling and signaling by a kinase switch. Proc. Natl. Acad. Sci. USA *110*, 15289–15294.

von Zastrow, M., and Williams, J.T. (2012). Modulating neuromodulation by receptor membrane traffic in the endocytic pathway. Neuron *76*, 22–32.

Williams, J.T., Ingram, S.L., Henderson, G., Chavkin, C., von Zastrow, M., Schulz, S., Koch, T., Evans, C.J., and Christie, M.J. (2013). Regulation of μ-opioid receptors: desensitization, phosphorylation, internalization, and tolerance. Pharmacol. Rev. *65*, 223–254.

Yu, Y.J., Arttamangkul, S., Evans, C.J., Williams, J.T., and von Zastrow, M. (2009). Neurokinin 1 receptors regulate morphine-induced endocytosis and desensitization of μ-opioid receptors in CNS neurons. J. Neurosci. *29*, 222–233.

Yu, Y.J., Dhavan, R., Chevalier, M.W., Yudowski, G.A., and von Zastrow, M. (2010). Rapid delivery of internalized signaling receptors to the somatodendritic surface by sequence-specific local insertion. J. Neurosci. *30*, 11703–11714.

Yudowski, G.A., Puthenveedu, M.A., and von Zastrow, M. (2006). Distinct modes of regulated receptor insertion to the somatodendritic plasma membrane. Nat. Neurosci. *9*, 622–627.

Yudowski, G.A., Puthenveedu, M.A., Henry, A.G., and von Zastrow, M. (2009). Cargo-mediated regulation of a rapid Rab4-dependent recycling pathway. Mol. Biol. Cell *20*, 2774–2784.

Cell Reports

Supplemental Information

Cell-Autonomous Regulation of Mu-Opioid Receptor Recycling by Substance P

Shanna L. Bowman, Amanda L. Soohoo, Daniel J. Shiwarski, Stefan Schulz, Amynah A. Pradhan, and Manojkumar A. Puthenveedu

Supplemental Figures and Legends

Figure S1

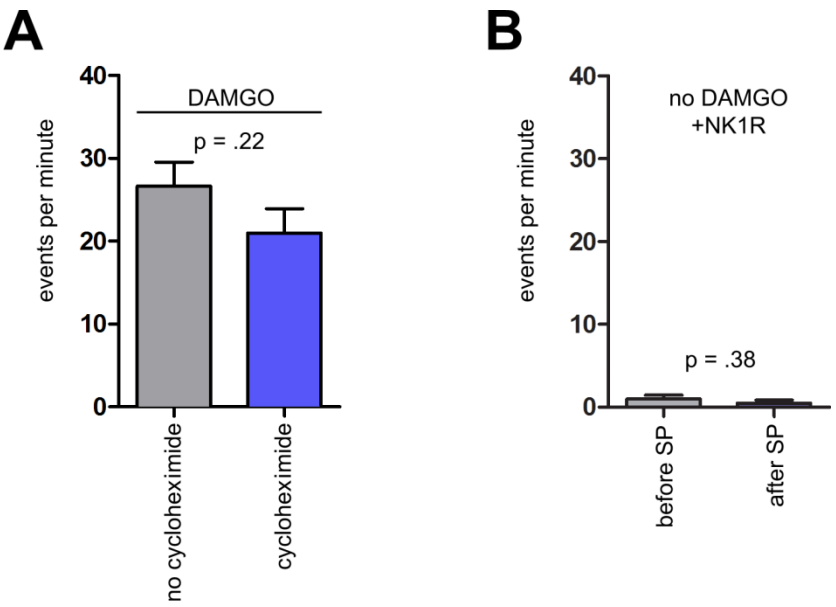

Fig S1. SpH-MOR Single event recycling assays are unaffected by changes in biosynthetic trafficking and NK1R trafficking, related to Fig 2.
A) HEK293 cells were either pre-treated with 10μM cyclohexamide for 4h at 37°C or not pre-treated with cyclohexamide, and incubated with DAMGO. Number of recycling events per minute after 5 min DAMGO incubation are plotted (n = 52, no treatment, n = 28, + cyclohexamide, error bars are s.e.m. across cells). B) Number of recycling events per minute before and after 5 min SP incubation (no DAMGO pre-treatment) are plotted, from HEK293 cells co-expressing SpH-MOR and HA-NK1R (n = 20, error bars are s.e.m. across cells).

Figure S2

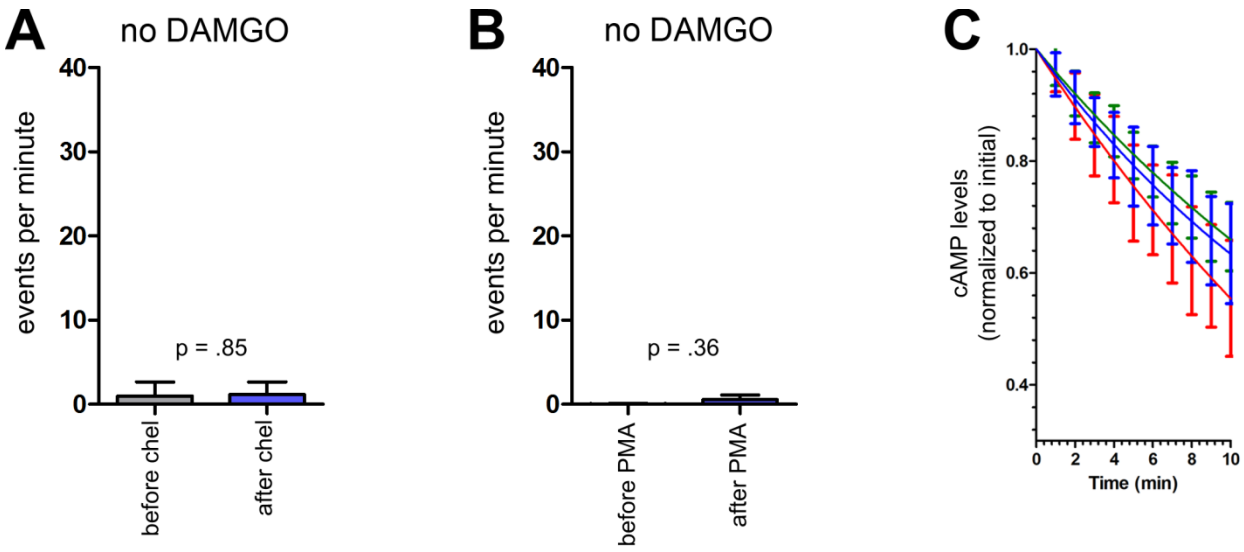

Fig S2. PKC inhibition or activation does not affect MOR recycling or signaling without the presence of agonist, related to Fig 3. A) Number of SpH-MOR recycling events per minute before and after 1 min chel addition in absence of DAMGO (n = 17 cells, error bars are s.e.m. across cells). B) Number of SpH-MOR recycling events per minute before and after 1 min PMA addition in absence of DAMGO (n = 6 cells, error bars are s.e.m. across cells). C). Luminescence-based cAMP detection assay, as in Fig 3B. Chel (green), PMA (blue), or vehicle (red) were added to cells before treatment with DAMGO. Chel and PMA pre-treatments did not affect the initial DAMGO challenge effect on cAMP levels (n = 3 separate experimental trials, error bars are s.e.m. across multiple trials.

Figure S3

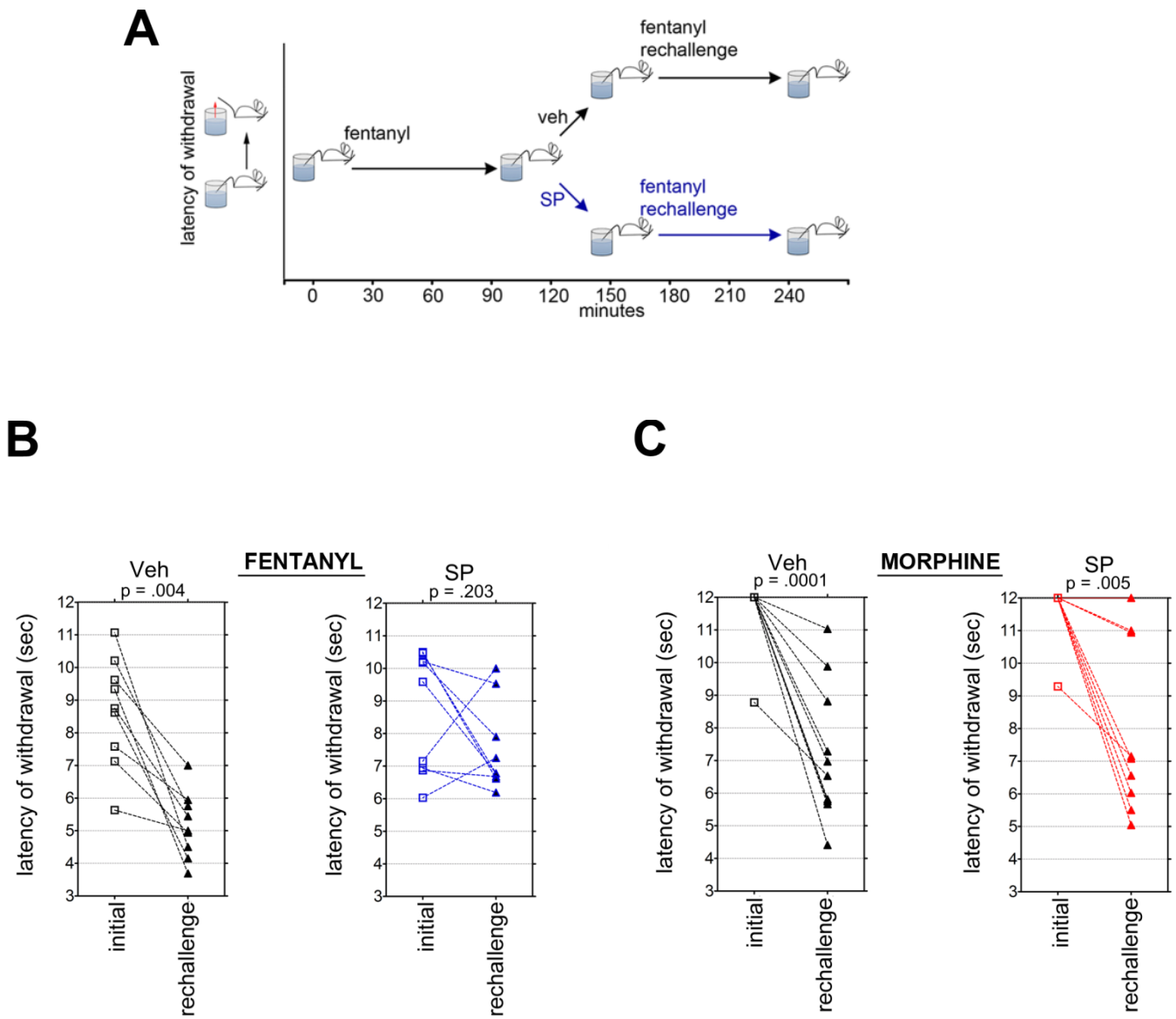

Fig S3. Design of thermal antinociception assay and paired responses from individual animals, related to Fig 7. A) Schematic of warm-water tail withdrawal assay. Baseline measurements were taken, animals were injected with agonist (fentanyl shown), and tail-withdrawal latencies were measured every 30 min. Saline (vehicle ctrl) or SP was injected intrathecally after initial response returned to baseline (120 min for fentanyl fentanyl; 210 min for morphine). B) Graph of responses of individual mice to initial fentanyl injection and rechallenge for vehicle ctrl and SP animals. C) Graph of responses of individual mice to morphine injection and rechallenge for vehicle ctrl and SP injected animals.

Supplemental Movie Legends

Movie S1. SpH-MOR individual exocytic events 5 min after DAMGO addition, related to Fig 2 A-C. An example cell expressing SpH-MOR imaged 5 min after DAMGO by TIR-FM at 10 frames per second. Movie is played in real time. Exocytic events appear as bright, concentrated puncta of fluorescence, followed by diffusion of the signal on the cell surface. See also Fig 2.

Movie S2. Lifetime of an individual SpH-MOR exocytic event, related to Fig 2 A-C. Exocytic events are characterized by a transient burst in maximum intensity (indicated in heat map of intensity) as vesicles fuse and SpH-MOR is dequenched by exposure to the external environment. Maximum intensity decreases as receptors diffuse across the cell membrane. Movie is shown at 3 frames per second (slowed down to a third of real time speed). See also Fig 2.

Movie S3. SpH-MOR exocytic events in HEK 293 cells expressing HA-NK1R, related to Fig 2 E. Adjacent cell (-NK1R) does not express HA-NK1R. Cells were imaged 5 min after DAMGO addition (-SP). SP was added, and cells were imaged 5 min later (+SP). Time of imaging is noted with respect to SP addition, movie is shown at 20 frames per second. See also Fig 2.